Dalton Transactions

ROYAL SOCIETY OF CHEMISTRY

PAPER

View Article Online
View Journal | View Issue

Cite this: *Dalton Trans.*, 2024, **53**, 17525

A synergetic effect of light and anion: near-infrared colorimetric monitoring of nitric oxide (NO) release from fluoride/cyanide anions and a water responsive ruthenium nitrosyl complex†

Nancy Sharma, Nitin, Srushti Gadiyaram, Amrita Ghosh and D. Amilan Jose *

Near-infrared (NIR) spectral-responsive multitasking chemical systems are always advantageous in biological and environmental systems. Although ruthenium complexes are highly attractive compounds for many applications, studies on NIR optical responsive sensors are very limited because of their synthetic difficulties. The sensing of fluoride and cyanide ions using ruthenium nitrosyl complexes is not known. In this study, we report the synthesis and characterization of a new terpyridine-based ruthenium nitrosyl complex $[Ru(Cl)_2NO(terpy\text{-}C_6H_4OH)]$ **1·Ru-OH**. The complex exhibited distinct NIR absorptions at 680 nm, as well as a visible color change with the fluoride ion in DMSO–CH_3CN medium. However, when the solvent is changed to DMSO–H_2O, it responds only with a cyanide ion with a distinct colorimetric change. Binding of the F^- ion leads to deprotonation of **1·Ru-OH**; the deprotonated complex is also used for the colorimetric detection of a trace amount of water in DMSO and acetonitrile with a limit of detection (LOD) of 0.034 wt% and 0.007 wt%, respectively. Ruthenium nitrosyl complexes have appeared as promising platforms for light-controlled release of nitric oxide (NO), which can be beneficial for therapeutic application. NO release studies of **1·Ru-OH** by UV-vis and FT-IR spectroscopy confirm that it can release NO in a light-controlled manner. In addition, the NO release could be monitored by the naked eye with a color change and spectral change in the NIR region. Importantly, NO release studies revealed that the rate of NO release could be modulated in the presence of the F^- ion. Here, the fluoride ion acts as an allosteric regulator. These results demonstrate that **1·Ru-OH** is both a promising multitasking colorimetric and NIR sensor and a colorimetric responsive NO-releasing agent.

Received 9th September 2024,
Accepted 1st October 2024

DOI: 10.1039/d4dt02576h

rsc.li/dalton

1. Introduction

Nitric oxide (NO) is an endogenous molecule, and several biological processes require NO as a signaling molecule to carry out their functions.[1] The deficiency of NO can disrupt biological pathways. Therefore, the exogenous delivery of NO could be a feasible possibility to overcome NO deficiency and for various medical benefits. NO-releasing donors and pro-drugs are considered as the best options for exogenous NO delivery in biological systems. The therapeutic beneficial effects of NO have encouraged researchers to develop novel NO-releasing molecules and materials that can locally release and deliver NO in a controlled manner. In this regard, ruthenium nitrosyl complexes have been considered prominent NO donors for the light-controlled release of NO due to their unique photophysical properties, low toxicity, easy modification of the ligand, and greater stability in solution.[2] Over the years, several reports have revealed light-triggered NO release from ruthenium nitrosyl complexes.[3–6] However, near-infrared (NIR) based colorimetric monitoring of NO release from ruthenium nitrosyl complexes is not known. The real-time monitoring and measurement of NO delivery and release is an important issue. Although several methods for the delivery and detection of NO are available, these are still very limited. Various spectroscopic and electrochemical methods such as EPR (NO spin trapping followed by spectrometry in a magnetic field), electrochemistry, colorimetry (Griess assay), and fluorometry (NO-specific fluorescent dyes) have been used to monitor the NO in biological systems. However, the efficiency of NO delivery could be compromised by detection technologies that consume NO. To overcome this issue, several fluorescent self-reporting NO-releasing molecules have been well documented.[7–13] Sortino *et al.* have reported a nitrobenzofurazan-based organic donor that exhibits fluorescence emission after releasing NO without the need for external fluorescent

Department of Chemistry, National Institute of Technology Kurukshetra, Kurukshetra-136119, Haryana, India. E-mail: amilanjosenit@nitkkr.ac.in

† Electronic supplementary information (ESI) available. See DOI: https://doi.org/10.1039/d4dt02576h

agents.[14] The same group also reported a series of several other fluorescent self-reporting NO-releasing molecules. However, the colorimetric self-reporting NO release probes that can be monitored by the naked eye with a visible colour change are not known in the literature. In addition to light, researchers have adopted various stimuli for releasing NO such as amino acids,[15] pH,[16] enzymes[17] and ultrasound[18] using metal and metal-free NO donors. Although light-induced controlled release of NO has been much explored, manipulation of the NO release measurement using an external regulator along with the encapsulation of the oxygen has not yet been explored. Usually, an external colorimetric reagent, such as the Griess reagent, is required to monitor the release of NO colorimetrically.[19] The use of an anion as an external regulator along with light has not been used to monitor the release of NO. Furthermore, the detection of biologically and environmentally relevant fluoride (F^-) and cyanide (CN^-) anions is of particular importance. The deficiency of fluoride can lead to osteoporosis and its excessive levels in water can cause skeletal fluorosis.[20] Cyanide, on the other hand, is very lethal to human health even at micromolar concentrations as it rapidly interacts with the active site of cytochrome oxidase and is also frequently utilized in various industrial and chemical applications.[21] Therefore, effective chemical sensors for their easy visual detection are required. Ruthenium(II) polypyridyl complexes have been reported for sensing cations and anions.[22,23] But the use of ruthenium nitrosyl complexes for anion sensing is rare; also, the effect of the anion on NO release with a colorimetric response is an added advantage and has not been reported in the literature.

Here, we describe a new ruthenium nitrosyl complex based on terpyridine phenol complexes $[Ru(Cl)_2NO(terpy\text{-}C_6H_4OH)]$ (**1·Ru-OH**), which releases NO under the control of blue-light irradiation. The hydroxyl group is part of a phenyl ring attached to the central terpyridine ring. Having a hydroxyl group, complex **1·Ru-OH** showed a binding behavior of fluoride (F^-) and cyanide (CN^-) depending on the solvent medium. The anion selectivity of **1·Ru-OH** with CN^- and F^- anions can be controlled in a selective solvent environment. **1·Ru-OH** is deprotonated by the F^- ion and acts as a colorimetric indicator to monitor NO release. The influence of anion binding on the NO release behavior was studied using the kinetics of NO release. To the best of our knowledge, this is the first example that describes the colorimetric monitoring of NO release in the NIR region by the binding of an anion along with light stimuli. Thus, this report describes a novel near-IR colorimetric sensor based on a ruthenium nitrosyl complex that releases therapeutic NO in a controlled manner.

2. Experimental section

2.1. Materials and reagents

2-Acetylpyridine, 4 hydroxybenzaldehyde, potassium pentachloronitrosylruthenate(II), ammonium hexafluorophosphate, tetrabutylammonium anion salts (F^-, Cl^-, Br^-, I^-, CN^-, CH_3COO^-) and the modified Griess reagent were purchased from Sigma-Aldrich. NH_3 solution, potassium bromide (IR spectroscopy) and NaOH pellets were purchased from Loba-Chemie. The 4-amino-5-methylamino-2′,7′-difluorescein diacetate (DAF-FM diacetate) NO detection kit was purchased from Thermo-Fisher Scientific. All of the solvents were of analytical grade and were used without further purification.

2.2. Synthesis of $[RuCl_2(NO)(terpy\text{-}C_6H_4OH)]$ (1·Ru-OH)

The ligand 4′-hydroxy-2,2′:6′,2″-terpyridine (**1**) was synthesized according to the procedure reported in the literature.[24] For **1·Ru-OH** synthesis, a solution of $K_2[RuCl_5(NO)]$ (180 mg, 0.46 mmol) and potassium chloride (447 mg, 5.99 mmol) dissolved in 10 ml of water was added to an ethanolic solution of ligand **1** (150 mg, 0.46 mmol). The reaction mixture was allowed to reflux in the dark for 3 hours. After cooling, golden-colored precipitates were filtered off, which turned black upon the addition of water. An aqueous NH_4PF_6 solution was added to the filtrate to obtain a brownish precipitate. It was filtered and washed with water, cold ethanol and diethyl ether, and dried completely *in vacuo*. Yield = 77 mg (25%). Anal. calcd for **1·Ru-OH**, $C_{41}H_{33}F_6N_4O_2PRu$ (M_w = 672.31): C 37.52, H 2.25, N 8.33, O 4.76. Found: C 37.48, H 2.29, N 8.31, O 4.90. IR (KBr): υ_{max} (cm^{-1}) 1901.81 (N–O), HR-MS: m/z $[M - PF_6]^+$: calcd 526.9614, found 526.9594. ^{1}H-NMR (DMSO-d_6, 500 MHz): δ (ppm) 10.64 (s, 1H), 9.18 (s, 2H), 9.16 (d, J = 6.3 Hz, 4H), 8.55 (t, J = 7.8 Hz, 2H), 8.27 (t, J = 8.4 Hz, 2H), 8.00 (t, J = 6.3 Hz, 2H), 7.09 (d, J = 8.5 Hz, 2H). ^{31}P-NMR (DMSO-d_6, 500 MHz): −140.6 (septet, PF_6) (see ESI Fig. S1–S4†).

2.3. NO release studies of 1·Ru-OH and 1·Ru-O$^-$ with light

UV-vis spectral changes were recorded for photoinduced NO release from **1·Ru-OH** and **1·Ru-O$^-$**. For this, a 2 mL solution of **1·Ru-OH** (43.3 μM) was prepared in a DMSO : CH_3CN (3 : 97) solvent system. The spectral changes were recorded upon irradiation with blue LED light (λ = 410 nm, 3 W) in a quartz cuvette of 1 cm path length. The absorption spectrum was recorded at different time intervals for 60 min. The light source was placed at a distance of 4 cm from the cuvette for all the irradiation experiments. 2 ml of **1·Ru-OH** (43.3 μM) in DMSO : CH_3CN (3 : 97) was added to $(butyl)_4N^+F^-$ (48 μM) to generate the deprotonated form of **1·Ru-OH**, designated as **1·Ru-O$^-$**. The UV-vis spectral changes of **1·Ru-O$^-$** were also recorded at different time intervals after photoirradiation with blue light in a quartz cuvette.

2.4. Anion-binding studies

The stock solutions of all anions were of 0.01 M concentration prepared in DMSO : CH_3CN (3 : 97) and DMSO. The solution of **1·Ru-OH** (43.3 μM) and anions (43.3 μM) such as F^-, Cl^-, Br^-, I^-, CN^-, and CH_3COO^- were added individually to each experiment and UV-vis spectral changes were recorded to observe the effect of the anions.

2.5. Titration of 1·Ru-OH with the F$^-$ ion

To determine the binding efficiency of fluoride ions, a 2 ml solution of **1·Ru-OH** (43.3 μM) was prepared in DMSO : CH_3CN

(3 : 97) or in DMSO. Titration was carried out with a 0.01 M stock solution of $(butyl)_4N^+F^-$. Different concentrations of F^- (0–60 μM) were successively added until saturation and the spectral changes were recorded.

2.6. Titration of 1·Ru-OH with the CN^- ion

For cyanide ion titration, 2 ml of **1·Ru-OH** (43.3 μM) was prepared in CH_3CN–H_2O (5/95%). Titration was carried out with a 0.01 M stock solution of $(butyl)_4N^+CN^-$. Different concentrations of CN^- (0–0.5 mM) were successively added and the spectral changes were recorded in a quartz cuvette.

2.7. FT-IR assay of 1·Ru-OH and 1·Ru-O^-

A time-dependent infrared (IR) study was performed for both **1·Ru-OH** and **1·Ru-O^-**. The IR stretching frequency υ(NO) at 1901 cm^{-1} was monitored upon irradiation with blue light at different time intervals. The deprotonation of **1·Ru-OH** with F^- and the irradiation experiment of the deprotonated form **1·Ru-O^-** were also checked with FT-IR spectroscopy.

3. Results and discussion

A terpyridine phenol based new ruthenium nitrosyl complex $[Ru(Cl)_2NO(terpy\text{-}C_6H_4OH)]$ (**1·Ru-OH**) with the Enemark–Feltham notation ($\{Ru\text{-}NO\}^6$) was prepared by reacting ligand **1** and $K_2[RuCl_5(NO)]$ in an EtOH–H_2O (3 : 1, v/v) mixture in the presence of KCl. Complex **1·Ru-OH** was isolated as its hexafluorophosphate salt (Scheme 1) as a brown powder in 25% yield. The purity of the complex was confirmed using standard analytical techniques such as ^{1}H-NMR, HR-MS, UV-vis and FT-IR spectroscopy (Fig. S1–S3†).

The terpyridine derivatives are known to coordinate with the metal center in a tridentate fashion leaving the two chloride ligands and one nitrosyl ligand. Therefore, there is a possible formation of geometric isomers of the **1·Ru-OH** complex, *trans* being the major isomer product as observed in the IR spectrum (Fig. S3†). The stretching frequency υ(NO) was observed at 1901 cm^{-1} which is close to the value reported by the Malfant group[25] for a similar type of *trans*-dichlorido species. It has been reported that, for a similar type of terpyridine-based ruthenium nitrosyl complex, the stretching vibration υ(NO) for the *cis*-dichlorido isomers ($[Ru(FT)Cl_2(NO)]^+$ = 1894 cm^{-1} and $[Ru(terpy)Cl_2(NO)]^+$ = 1860 cm^{-1}) is lower as compared to the *trans*-dichlorido isomers ($[Ru(FT)Cl_2(NO)]^+$ = 1901 cm^{-1} and $[Ru(terpy)Cl_2(NO)]^+$ = 1895 cm^{-1}) in FT-IR spectroscopy.[25,26] As the solvent molecules could easily replace the chloride ligands present *trans* to the NO ligand in $[RuCl_5NO]^{2-}$, the major product formed would be the *trans*-dichlorido isomer.[26,27] The preparation and separation of *cis* and *trans* isomers and their single crystal X-ray diffraction structures of similar type complexes have already been documented.[25,27–30] Complex **1·Ru-OH** was used as such and the isomers were not separated; all studies were performed without any separation of geometric isomers. The high-resolution (HR) mass spectrum confirms the presence of a single charged cation peak $[RuCl_2(NO)(1)]^+$ at m/z = 526.9594 which is close to the value obtained with the theoretical isotopic pattern *i.e.*, m/z = 526.9614 (Fig. S1†).

3.1. Anion binding and deprotonation of 1·Ru-OH

Phenol-based derivatives are well known to interact with anions and undergo deprotonation in the presence of basic anions such as cyanide or fluoride through the Brønsted acid–base reaction mechanism.[31] Deprotonation results in a colorimetric or emission response due to the transformation of the phenolic group into its phenolate ion.[32] The abstraction of a proton from the phenol group by a basic anion leads to this transformation. When this point was considered, terpyridine was modified to synthesize ligand **1** and the ruthenium nitrosyl complex with an anionic binding site (**1·Ru-OH**) was prepared. The spectral changes of **1·Ru-OH** in the presence of different anions (F^-, Cl^-, Br^-, I^-, CN^-, CH_3COO^-) were recorded in a 3% DMSO : 97% CH_3CN system. As shown in Fig. 1(A), a prominent UV-vis spectral change in the NIR region of the spectra was observed only in the case of F^- with a significant color change from yellow to blue as seen in Fig. 1(B).

The UV-vis absorption spectrum of **1·Ru-OH** in 3% DMSO : CH_3CN (3/97%) showed intense absorption bands at 410 nm, 345 nm, and 280 nm. **1·Ru-OH** showed similar absorption bands in a DMSO solvent system as well. Due to the addition of $(butyl)_4N^+F^-$ (0–60 μM) to **1·Ru-OH**, the absorption band at 410 nm decreased and a new broad absorption band appeared in the near-IR region at 680 nm along with a color change. The three isosbestic points obtained at 457, 371 and 312 nm indicate the possible formation of an immediate transient **1·Ru-OH···F^-** complex leading to the stable formation of its deprotonated form **1·Ru-O^-** (Fig. 2A and B). The

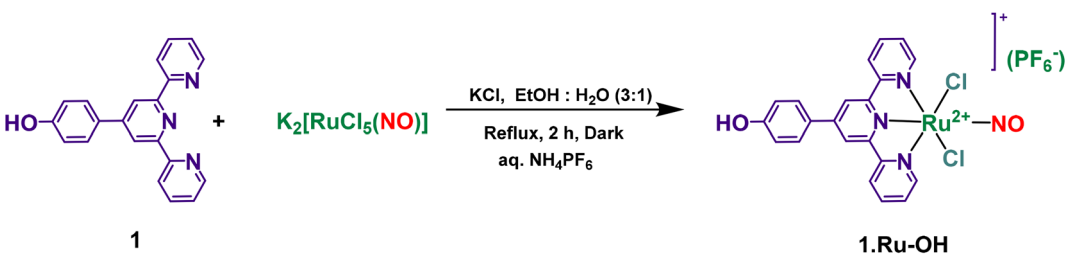

1 1.Ru-OH

Scheme 1 Schematic representation for the synthesis of **1·Ru-OH**.

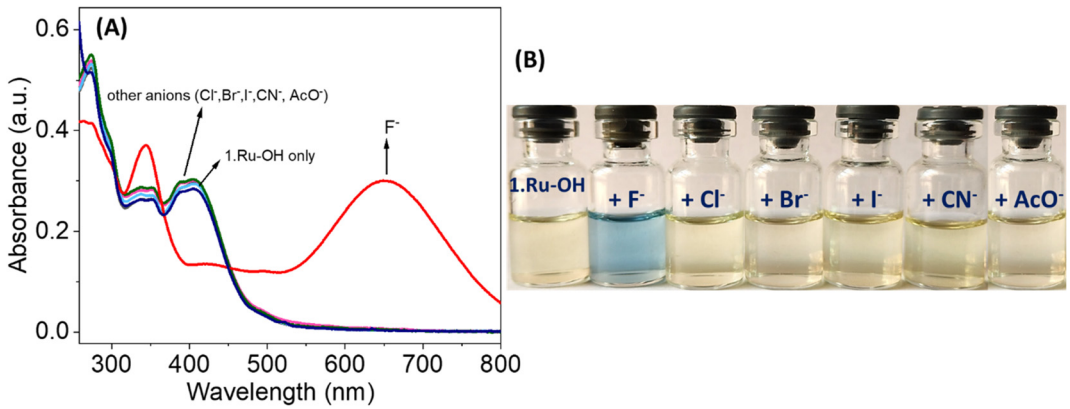

Fig. 1 (A) Changes in the absorption spectra of **1·Ru-OH** (43.3 μM) in the presence of various analytes such as F^-, Cl^-, Br^-, I^-, CN^-, and CH_3COO^- (43.3 μM) in a DMSO : CH_3CN (3 : 97) system. (B) Colorimetric response of **1·Ru-OH** in the presence of different anions.

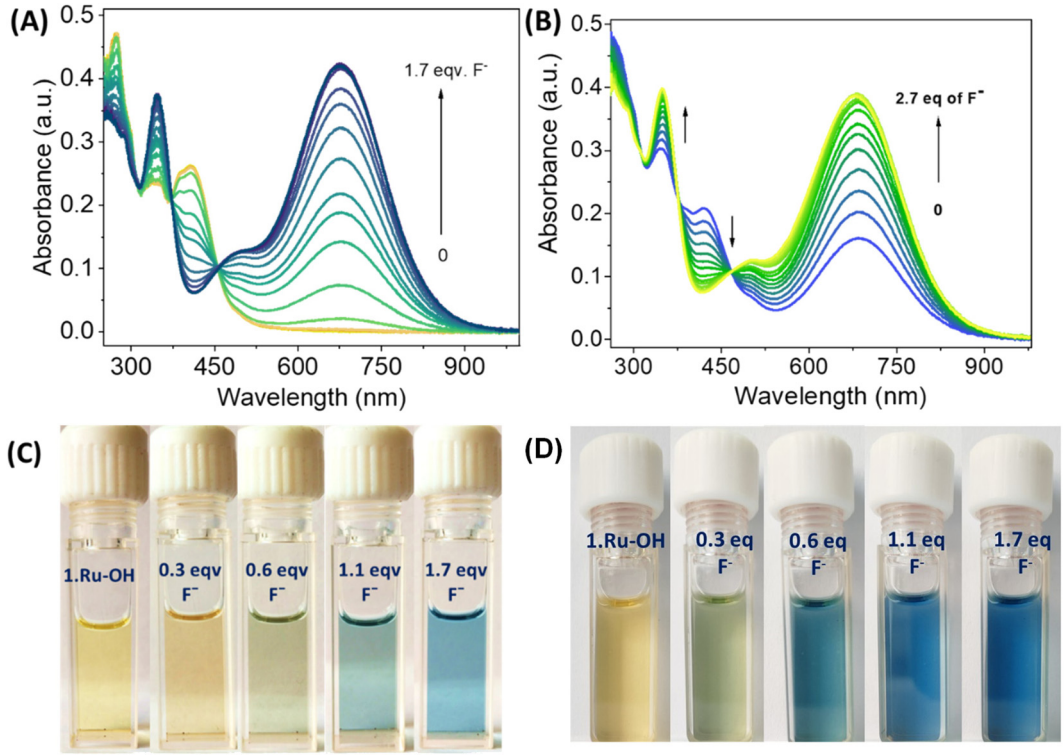

Fig. 2 (A) UV-vis titration of **1·Ru-OH** (43.3 μM) with increasing amounts of $(butyl)_4N^+F^-$ (0–60 μM) in a DMSO : CH_3CN (3 : 97) system. (B) UV-vis titration of **1·Ru-OH** (43.3 μM) with increasing amounts of $(butyl)_4N^+F^-$ (0–120 μM) in pure DMSO. (C) Colorimetric monitoring of the deprotonation of **1·Ru-OH** in a DMSO : CH_3CN (3 : 97) mixture. (D) Colorimetric monitoring of the deprotonation of **1·Ru-OH** in DMSO.

colorimetric response of the probe due to the formation of the phenolate ion was visually traced (Fig. 2C and D). In the presence of F^-, **1·Ru-OH** forms an intermolecular H bond with F^- and then undergoes deprotonation, due to the electronic properties of the ruthenium complex being altered. Deprotonation leads to extensive π-delocalization in the terpyridine moiety, resulting in the appearance of a new band in the NIR region with a color change from yellow to blue. The F^- sensing behavior of the phenol-based metal complex is already known in an organic medium.[32] Other anions did not produce any such change due to weak interactions with the phenolic group (–OH) in the organic medium.

The bindings constants were calculated *via* the Hill plot (concentration *vs.* change in absorbance) and were found to be 4.11×10^4 M^{-1} and 7.56×10^4 M^{-1} in CH_3CN and DMSO, respectively (Table 1). The limit of detection (LOD) by the linear plot was calculated as 0.24 μM and 0.48 μM in CH_3CN and DMSO, respectively. The binding constant and LOD of a probe in DMSO were twice the values in CH_3CN, indicating a better binding of F^- in CH_3CN. The LOD of F^- in the case of acetonitrile is possibly

Table 1 The binding constants and the detection limits of receptors **1·Ru-OH** and **1·Ru-O$^-$**

Receptor	Solvent	Binding constant	Detection limit (LOD)
1·Ru-OH (with F^-)	CH_3CN	$4.11 \times 10^4\ M^{-1}$	0.24 μM
	DMSO	$7.56 \times 10^4\ M^{-1}$	0.48 μM
1·Ru-O$^-$ (with H_2O)	CH_3CN	—	0.007 wt%
	DMSO	—	0.034 wt%

better due to the involvement of the solvent in complex formation.[33] Thus the UV-vis results confirm the use of **1·Ru-OH** for the selective detection of the F^- ion in the NIR region. In organic solvents, the highly electronegative F^- ion has a higher affinity for H bonding with the –OH group of **1·Ru-OH** than the other anions, which shows a significant red-shift towards the NIR region.[34] The selective detection of F^- over other anions, characterized by a significant bathochromic shift with the appearance of a new peak in the near-IR region, shows certain potential for applications in biological systems. The binding constant and detection limits calculated through the systematic absorption titrations are tabulated below.

As described earlier by us and others,[35,36] the deprotonated species can be used as water/moisture sensors using water which can reprotonate the probe. Because anion-induced deprotonated species are not very stable in aqueous media, even trace amounts of water can revert the deprotonation.[32] Therefore, the deprotonated form of **1·Ru-OH** designated as **1·Ru-O$^-$** was explored with water to work as a colorimetric moisture sensor by reprotonation. The sensitivity of **1·Ru-O$^-$** for the detection of water was determined by systematic UV-vis absorption titrations. Studies were carried out in CH_3CN and DMSO solvent systems with increasing concentrations (weight%) of water. The binding of F^- to neutral molecules in protic or aqueous solvents is not regular, since the solvation energy of F^- ions is very high in water.[37] This can be seen in Fig. 3A and B, where the saturation in the titration profile is only observed in the case of acetonitrile. In the case of water titrations, the changes are more prominent in acetonitrile media than in more polar DMSO.

The absorbance band at *ca.* 680 nm decreased with increasing amounts of water (0–10 weight%), and changes in the absorption spectra were observed along with the isosbestic points at around 420 and 350 nm (Fig. 3A and B). The color of

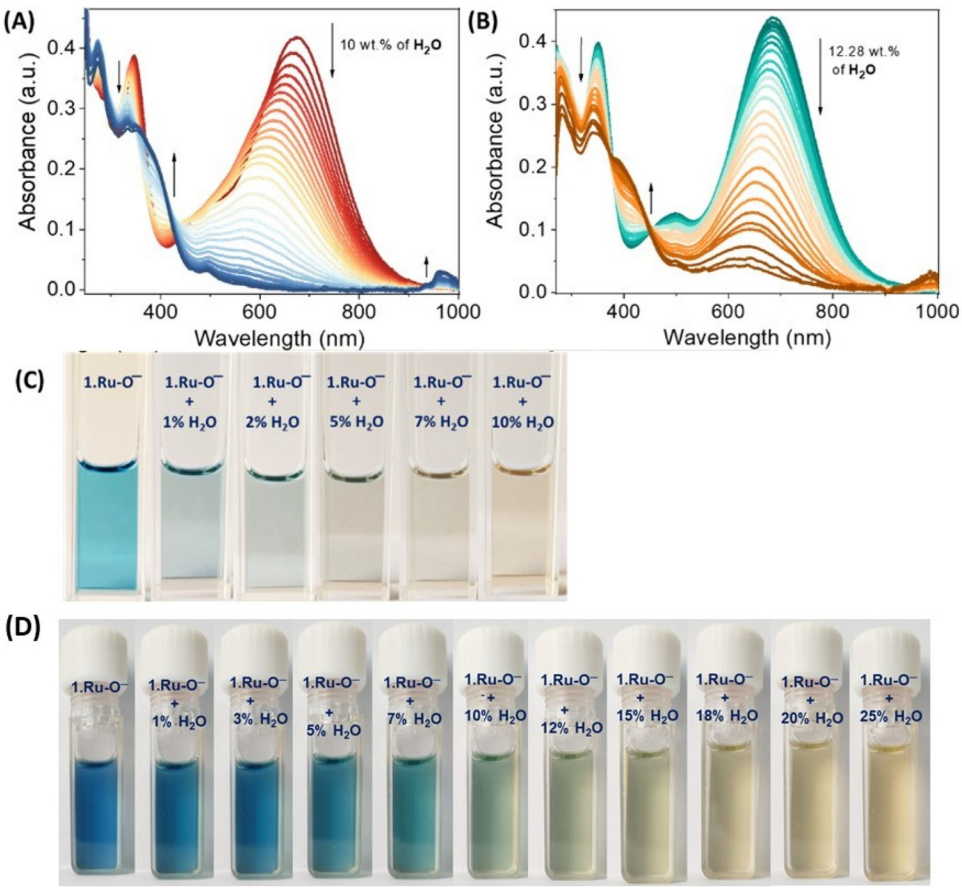

Fig. 3 (A) UV-vis absorption titration of **1·Ru-O$^-$** with increasing amounts of water (0–10 weight%) in a DMSO : CH_3CN (3 : 97) system. (B) UV-vis absorption titration of **1·Ru-O$^-$** with increasing amounts of water (0–10 weight%) in DMSO. (C) Naked eye detection of reprotonation of **1·Ru-O$^-$** with water in acetonitrile. (D) Colorimetric monitoring of reprotonation of **1·Ru-O$^-$** with water in DMSO.

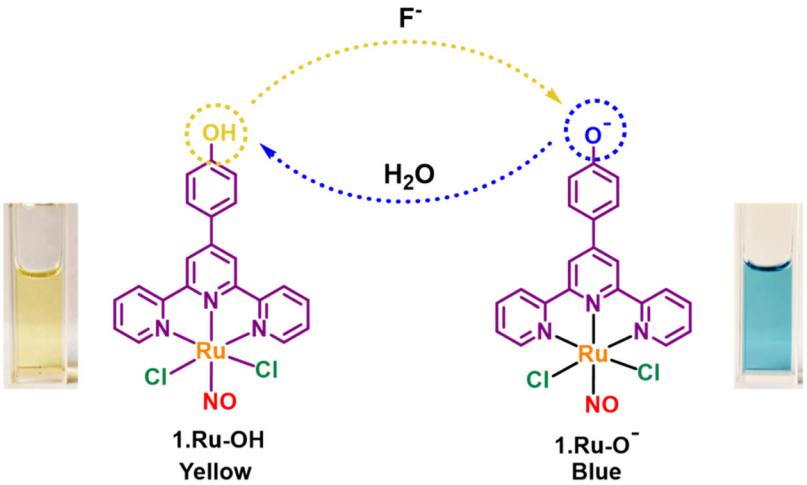

Scheme 2 The proposed mechanism for the detection of water by **1·Ru-O$^-$**.

1·Ru-O$^-$ was also affected by the sequential addition of water, and the color changed from blue to yellow as **1·Ru-OH** formed, indicating that the reprotonation could be monitored with the naked eye (Fig. 3C and D). The changes showed that **1·Ru-O$^-$** was reprotonated with the addition of water and the spectra showed a similarity with **1·Ru-OH**. Based on the changes in the spectra and the colorimetric change, a mechanism was proposed as shown in Scheme 2. With the help of UV-vis titrations, the LOD of water for the receptor was calculated as 0.007 weight% and 0.034 weight% in CH_3CN and DMSO, respectively (Table 1). The LOD of **1·Ru-O$^-$** in CH_3CN was almost five times better than that of DMSO.

The phenomenon of deprotonation of **1·Ru-OH** was also observed in a 95% aqueous system. For this, the spectral changes of **1·Ru-OH** in the presence of different anions (F^-, Cl^-, Br^-, I^-, CN^-, CH_3COO^-) were recorded in a 5% $CH_3CN:H_2O$ solution. As seen in Fig. 4A and B, significant changes were observed only in the case of CN^- with a change in color from yellow to violet. The UV-vis absorption spectrum of **1·Ru-OH** in a 5% $CH_3CN:H_2O$ solution showed intense absorption at 383 nm. Upon the addition of $(butyl)_4N^+CN^-$ (0–0.5 mM) to **1·Ru-OH**, the absorption band at 383 nm decreased and a new absorption band appeared at around 470 nm along with a color change as observed in Fig. 4B.

Systematic titration of **1·Ru-OH** with $(butyl)_4N^+CN^-$ was performed in $CH_3CN:H_2O$ (5 : 95%) solution. With the gradual addition of CN^- (0–1 equiv.) to **1·Ru-OH**, a decrease in absorbance at 383 nm was observed possibly due to the participation of CN^- in the interaction with the –OH group. With the excess addition of CN^- (1–12 equiv.), a new band appeared at 470 nm. The gradual change in color from yellow to orange to purple was observed with continuous addition of CN^- (Fig. 5A and B). The LOD for CN^- in aqueous media was calculated using the linear plot and was found to be 4.47 μM. The binding constant for CN^- calculated using the Hill plot was found to be 1.04×10^4 M^{-1} in a 5% $CH_3CN:H_2O$ solution. The colorimetric response of **1·Ru-OH** with the CN^- ion is due to the deprotonation of **1·Ru-OH**. The cyanide ion binds to H-bond donors (OH) by association with hydrogen atoms, which ultimately can lead to deprotonation of **1·Ru-OH**.[38] On deprotonation of the

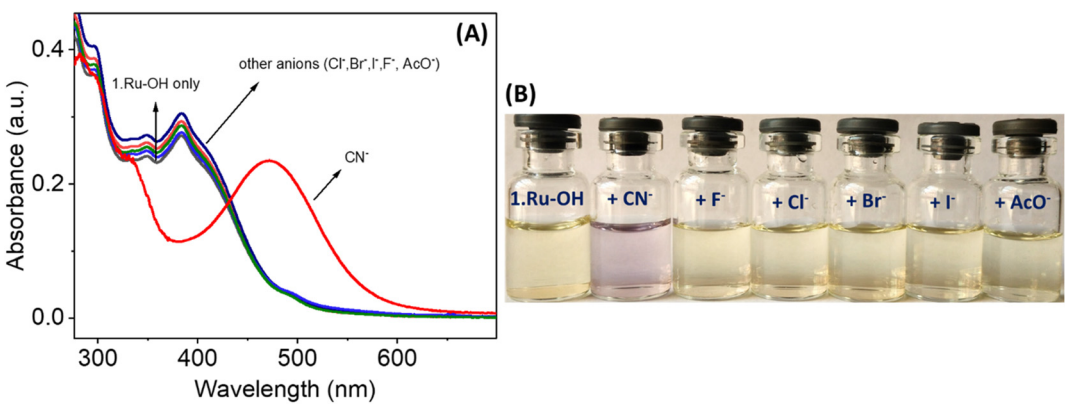

Fig. 4 (A) Changes in the absorption spectra of **1·Ru-OH** (43.3 μM) in the presence of various analytes such as F^-, Cl^-, Br^-, I^-, CN^-, and CH_3COO^- (4 equiv.) in a 5% CH_3CN : 95% H_2O solution. (B) Colorimetric response of **1·Ru-OH** in the presence of different anions.

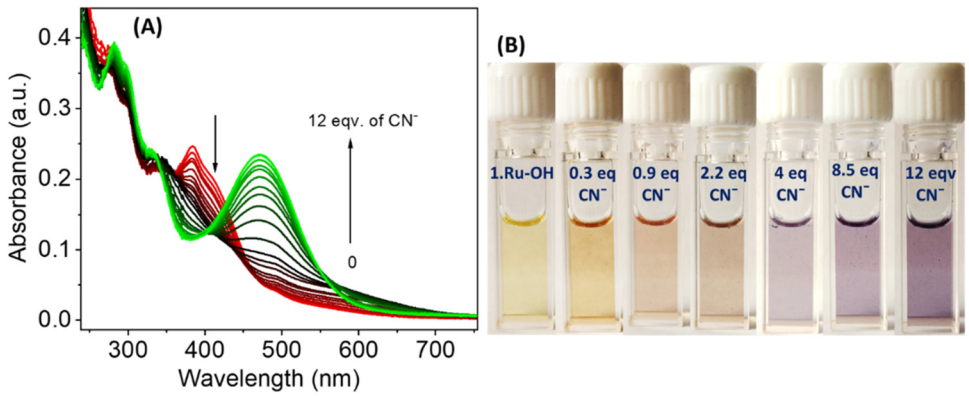

Fig. 5 (A) UV-vis titration of **1·Ru-OH** (43.3 μM) with increasing amounts of $(butyl)_4N^+CN^-$ (0–0.5 mM) in a solution of 5% $CH_3CN : H_2O$. (B) Colorimetric monitoring of **1·Ru-OH** in a 5% $CH_3CN : H_2O$ solution after the gradual addition of $(butyl)_4N^+CN^-$.

hydroxyl group, electron donation to the metal center is expected and can be visualized by resonance structures. This additional electron-donating character upon deprotonation changes the reduction potential of ruthenium to a greater extent, which leads to the color change of the solution.[39] From the above observations, it is clear that **1·Ru-OH** shows solvent-specific binding with different analytes. In pure organic media, **1·Ru-OH** binds to F^- ion whereas in an aqueous solution, CN^- is selectively binding the complex. The possible difference in the binding abilities of F^- and CN^- in organic and aqueous media, respectively, was due to the difference in the hydration energy. A higher nucleophilicity and a lower hydration energy were observed in the case of CN^- ($\Delta H_{Hyd} = -67$ kJ mol^{-1}) than in the case of F^- ($\Delta H_{Hyd} = -505$ kJ mol^{-1}) which explains the selectivity of CN^- in aqueous media.[34] Thus, due to the stronger nucleophilic nature and lower heat of hydration of CN^-, it interacts with the –OH group more preferentially than F^- in the case of a polar aqueous medium.

3.2. Photoinduced NO release study of 1·Ru-OH

NO is a monodentate ligand and coordinates with transition metals through a nitrogen atom as the donor and forms metal nitrosyl complexes. Most of the metal nitrosyl complexes are photolabile and release nitric oxide (NO) in the presence of certain light in the wavelength range of 250–800 nm. The wavelength of light could be modulated by altering the functionalization of the coordinated ligands. Most of the metal nitrosyl-based complexes, with the MLCT transition, lie in the biologically harmful UV range. By modifying the conjugation in the ligand, this transition could be pushed to the visible or even NIR range.[2] Among the metal-nitrosyl donors, ruthenium nitrosyl complexes are promising candidates because of their ability to mimic the coordination behavior of Fe in the biological environment. Ruthenium, being a 4d transition metal, mostly forms low-spin complexes (+2 and +3 oxidation states), which show lower lability compared to its 3d transition metal counterpart (Fe). Moreover, ruthenium complexes show low cytotoxicity, good stability, and good water solubility, and are photoactive. Due to these properties, ruthenium nitrosyl complexes functionalized with different ligands have been explored for photocontrolled NO release with light of different wavelengths.[40,41] Here, we have used a phenol derivative of terpyridine as the tridentate ligand that accounts for the robust binding with the ruthenium metal.

The UV-vis absorption spectrum of **1·Ru-OH** in acetonitrile showed the characteristic MLCT band of ruthenium at 410 nm, which may be attributed to the $d\pi(Ru) \rightarrow \pi^*(NO)$ transition. The intense absorption band at 280 nm is due to the terpyridine based $n \rightarrow \pi^*$ transition while the absorption band at 340 nm could presumably be due to $\pi \rightarrow \pi^*$ of the polypyridine ligands.[42] The change in the UV-Vis spectrum of **1·Ru-OH** (43.3 μM) in the DMSO/CH_3CN system (3 : 97) was monitored under blue light irradiation (=410 nm, 3 W) at different time intervals for 60 min to observe the photoinduced NO release ability of the ruthenium complex. The decrease in absorbance at 410 nm and the increase in absorbance at 318 nm and 498 nm with clear isosbestic points at 356 nm and 462 nm indicate the possible phototransformation of **1·Ru-OH** into its single photolyzed species (Fig. 6A). However, no such changes were observed when the solution was kept in the dark (Fig. 6B). The NO release kinetic experiment gave a rate constant of 1.515 min^{-1} with a half-life ($t_{1/2}$) of 30 s. The quantum yield value calculated for the release of nitric oxide (NO) from **1·Ru-OH** was found to be 0.016.[43]

To confirm the light-induced NO release, a time-dependent FT-IR assay was performed. For that, the solution of **1·Ru-OH** was kept under blue light for photolysis. Some aliquots of the samples were taken at different intervals of time and the solvent was removed under vacuum, and the solid residues obtained were analyzed by IR spectroscopy using the KBr pellet method. The peak of NO stretching υ(NO) observed at 1901 cm^{-1} for **1·Ru-OH** reduced significantly upon prolonged irradiation (Fig. 6C). These experiments further confirm the photoinduced NO release from the new ruthenium nitrosyl complex **1·Ru-OH**.

3.3. Photoinduced release of NO by 1·Ru-O$^-$

The H-bonding interaction between the –OH group of **1·Ru-OH** and the ion F^- was observed at lower concentrations of F^-.

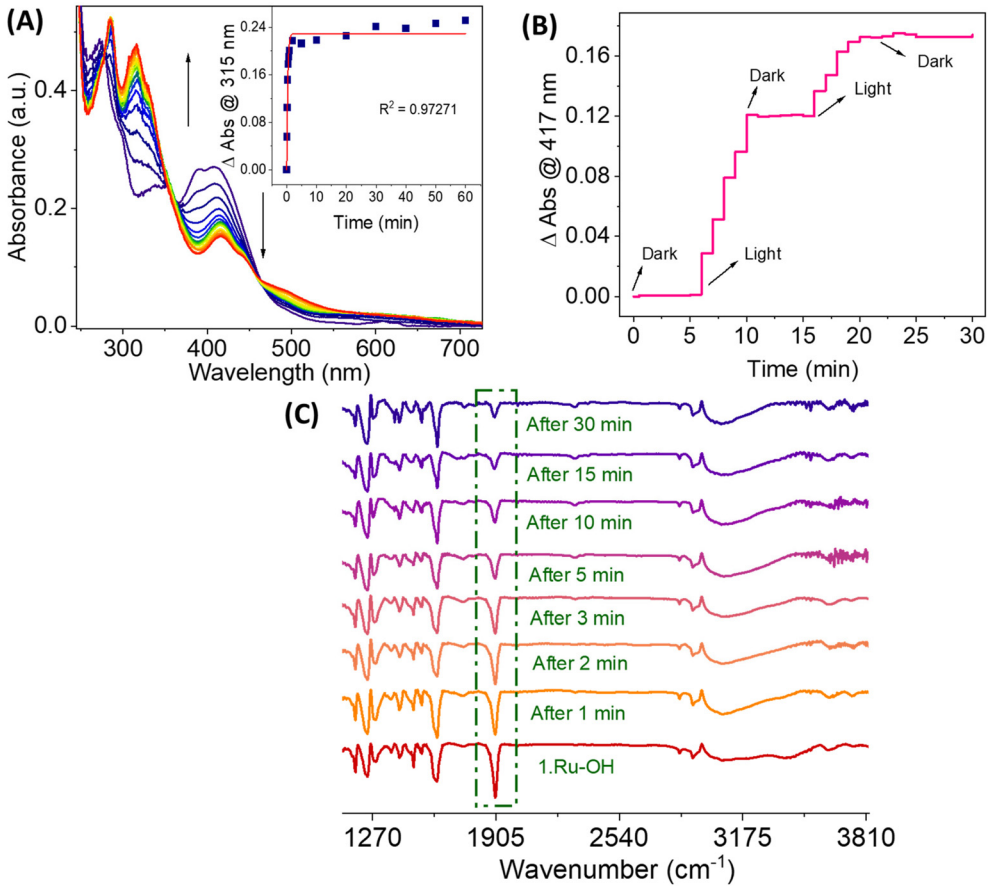

Fig. 6 (A) Photoirradiated absorption spectra of **1·Ru-OH** when irradiated with blue light (λ = 410 nm, 3 W). Inset: change in abs. *vs.* time at 315 nm. (B) Light and dark experiment with **1·Ru-OH**. (C) Time-dependent FT-IR spectrum of **1·Ru-OH** upon blue light irradiation.

However, at higher concentrations, the F^- ion causes deprotonation *via* Brønsted acid–base interactions.[44] To check the effect of deprotonation on the NO release behavior of **1·Ru-OH**, higher concentrations of F^- ions (48 μM) were used to deprotonate the receptor to form **1·Ru-O$^-$**, which was used for further studies. Time-dependent changes in the UV-vis spectra of the deprotonated form **1·Ru-O$^-$** were recorded with blue light at different time intervals for 60 minutes. Upon light irradiation, the disappearance of the absorption band at 680 nm and the appearance of a new band at 502 nm were observed.

In addition, an increase in absorbance was observed at 315 nm with a clear isosbestic point at 337 nm (Fig. 7A). The appearance of a new band at 502 nm could be due to the transformation of **1·Ru-O$^-$** into its photolyzed solvated species. The color of the deprotonated solution of **1·Ru-O$^-$** changed from blue to pink upon light irradiation (Fig. 7B). The release of NO from the deprotonated form of **1·Ru-OH**, *i.e.*, **1·Ru-O$^-$**, could be visualized with the naked eye. However, this was not the case for **1·Ru-OH** as there was no such colorimetric visualization of NO release. Therefore, the combined effect of anion and light leads to the colorimetric release of NO from **1·Ru-O$^-$**. The calculated rate constant for NO release (k_{NO}) from **1·Ru-OH** in the presence of F^- (48 μM) was found to be 0.553 min^{-1} with a half-life ($t_{1/2}$) of 1.25 min, which is slightly slower compared to the rate constant observed in the absence of F^- (k_{NO} = 1.515 min^{-1}). Based on these experimental results, it can be concluded that the deprotonated form of **1·Ru-OH** showed a longer half-life ($t_{1/2}$ = 1.25 min) compared to its protonated form ($t_{1/2}$ = 0.5 min). Binding of F^- to **1·Ru-OH** at one site could decrease the rate of NO release from the other site (Table 2). This concept is similar to the bio-like allosteric regulatory mechanism in which F^- acts as a negative allosteric regulator and decreases the affinity at the other site.

The NO release behavior of **1·Ru-O$^-$** was also confirmed by the FT-IR assay. As seen in Fig. 8, after the addition of $(butyl)_4N^+F^-$ (2 equiv.) to **1·Ru-OH** (1 mM), the –OH band at ~3400 cm^{-1} disappeared possibly due to the participation of the –OH group in H bonding with F^- which confirms the immediate formation of the deprotonated form **1·Ru-O$^-$**. The peak of NO at 1901 cm^{-1} in the IR spectrum of **1·Ru-O$^-$** started to disappear with regular intervals of blue-light irradiation. The peak completely disappeared after 40 min, confirming that the deprotonated form of **1·Ru-OH** also releases NO in the presence of light with a color change as observed in Fig. 7B. However, no such color change was observed when **1·Ru-O$^-$**

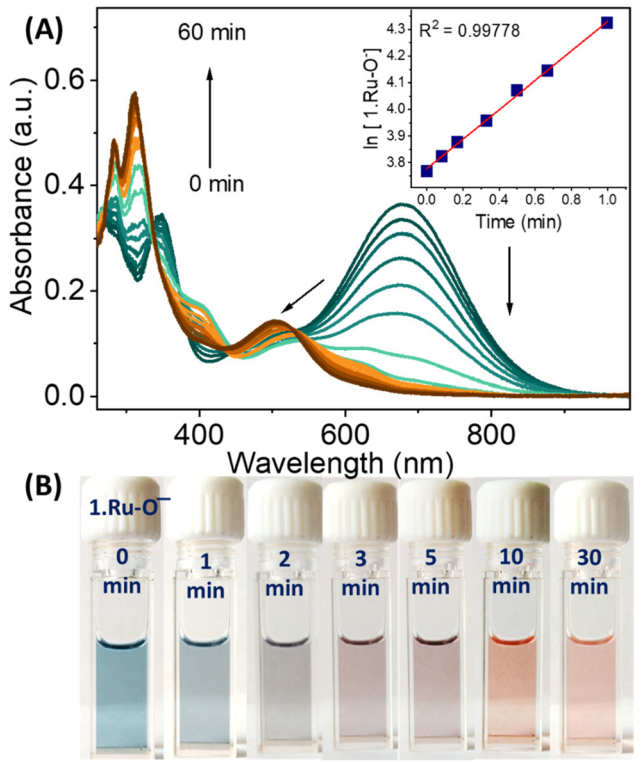

Fig. 7 (A) Time-dependent UV-vis absorption spectra of **1·Ru-O⁻** when irradiated with blue light (λ = 410 nm, 3 W). Inset: ln[**1·Ru-O⁻**] *vs.* time at 315 nm. (B) Colorimetric monitoring of NO release from **1·Ru-O⁻** upon addition of F^- ions (48 μM).

Table 2 Comparison of the NO release rate

Complex	Rate constant (k_{NO})	Half-life ($t_{1/2}$) of NO release	Quantum yield
1·Ru-OH	1.515 min^{-1}	0.5 min	1.6×10^{-2}
1·Ru-O⁻ (deprotonated form)	0.553 min^{-1}	1.25 min	0.6×10^{-2}

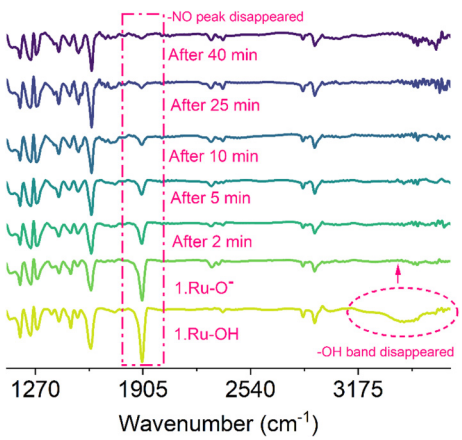

Fig. 8 Time-dependent FT-IR spectrum of **1·Ru-O** after blue light irradiation.

was kept in the dark. This result confirms the colorimetric monitoring of NO release from the NO donor **1·Ru-O⁻**; the NO release was easily monitored by the naked eye with a color change from purple to pink, as shown in Fig. 7B. To the best of our knowledge, such colorimetric monitoring of light-induced NO release is not known in the literature.

Consequently, binding of F^- (48 μM) to **1·Ru-OH** alters the apparent rate constant for NO release. The deprotonated form of the ruthenium nitrosyl complex, **1·Ru-O⁻**, shows slow release of nitric oxide with a longer half-life compared to its parent complex.

4. Conclusions

In this report, a new ruthenium nitrosyl complex [$Ru(Cl)_2NO$(terpy-C_6H_4OH)] (**1·Ru-OH**) has been prepared and characterized. The complex displayed anion binding behavior with F^- and CN^- in the DMSO–CH_3CN and DMSO–water solvent systems with a colorimetric response in the NIR region. The optical discrimination between the selectivity of CN^- and F^- using **1·Ru-OH** was achieved by changing the solvent medium. In an aqueous solvent system, **1·Ru-OH** selectively detects CN^-, whereas in a pure organic medium, it detects only the F^- ion. In the presence of excess F^- ions in an organic medium, the –OH group of the complex is deprotonated, and the deprotonated complex is also explored for the detection of a trace amount of water in DMSO and CH_3CN. Furthermore, the anion-responsive nitrosyl complex **1·Ru-OH** also showed an NO release property upon irradiation with blue light (λ = 410 nm, 3 W), which was confirmed by time-dependent FT-IR studies and UV-vis kinetics. The NO release behavior of **1·Ru-OH** in the presence of F ions was also checked. It was observed that with the F ion, in the deprotonated form, complex **1·Ru-OH** displayed a slightly slow NO release compared to the nondeprotonated form. However, the time-dependent NO release from deprotonated **1·Ru-OH** is easily monitored with the naked eye. A color change from blue to pink was observed upon NO release without the need for any external probe. But this was not the case with **1·Ru-OH** without an anion. This observation leads to a novel NO release system which responds to anions. The anion binding also plays an important role in modulating the NO release, and it helps to monitor the NO release by the naked eye. Therefore, the anion binding is combined with light to monitor the NO release by colorimetric change.

Data availability

The data supporting this article have been included as part of the ESI.†

Conflicts of interest

The authors declare no competing interests.

Acknowledgements

DAJ acknowledges the Science and Engineering Research Board (SERB), New Delhi, Core Research grant no. CRG/2022/004990, the Haryana State Council of Science Innovation and Technology (HSCSIT), Haryana for Grant no. HSCSIT/R&D/2022/2949 and CSIR-India for the CSIR-EMR(II) grant no. 01/3127/23/EMR-II.

References

1 D. A. Wink and J. B. Mitchell, *Free Radicals Biol. Med.*, 1998, **25**, 434–456.
2 I. Stepanenko, M. Zalibera, D. Schaniel, J. Telser and V. B. Arion, *Dalton Trans.*, 2022, **51**, 5367–5393.
3 B. Giri, T. Saini, S. Kumbhakar, K. Selvan K, A. Muley, A. Misra and S. Maji, *Dalton Trans.*, 2020, **49**, 10772–10785.
4 M. A. Crisalli, L. P. Franco, B. R. Silva, A. K. M. Holanda, L. M. Bendhack, R. S. Da Silva and P. C. Ford, *J. Coord. Chem.*, 2018, **71**, 1690–1703.
5 R. Kumar, S. Kumar, M. Bala, A. Ratnam, U. P. Singh and K. Ghosh, *RSC Adv.*, 2016, **6**, 72096–72106.
6 Y. Juarez-Martinez, P. Labra-Vázquez, A. Enríquez-Cabrera, A. F. Leon-Rojas, D. Martínez-Bourget, P. G. Lacroix, M. Tassé, S. Mallet-Ladeira, N. Farfán, R. Santillan, G. Ramos-Ortiz, J.-P. Malval and I. Malfant, *Chem. – Eur. J.*, 2022, **28**, e202201692.
7 A. Fraix, C. Parisi, M. Seggio and S. Sortino, *Chem. – Eur. J.*, 2021, **27**, 12714–12725.
8 Q. Guo, Y. Wu, L. Zhang, Y. Qin, J. Bao, Y. Feng, Y. Liu and Y. Zhou, *Sens. Actuators, B*, 2022, **369**, 132309.
9 C. Parisi, M. Failla, A. Fraix, B. Rolando, E. Gianquinto, F. Spyrakis, E. Gazzano, C. Riganti, L. Lazzarato, R. Fruttero, A. Gasco and S. Sortino, *Chem. – Eur. J.*, 2019, **25**, 11080–11084.
10 G. Ravikumar, M. Bagheri, D. K. Saini and H. Chakrapani, *ChemBioChem*, 2017, **18**, 1529–1534.
11 N. Ieda, M. Kawaguchi and H. Nakagawa, *Chem. Pharm. Bull.*, 2023, **71**, 447–450.
12 D. Saitoh, A. Suzuki, N. Ieda, Z. Liu, Y. Osakada, M. Fujitsuka, M. Kawaguchi and H. Nakagawa, *Org. Biomol. Chem.*, 2023, **21**, 2983–2989.
13 H. Thomsen, N. Marino, S. Conoci, S. Sortino and M. B. Ericson, *Sci. Rep.*, 2018, **8**, 1–8.
14 M. Seggio, S. Payamifar, A. Fraix, E. Kalydi, P. Kasal, O. Catanzano, C. Conte, F. Quaglia and S. Sortino, *New J. Chem.*, 2021, **45**, 8449–8455.
15 C. Zhang, X. Meng, C. Gong, J. Zhao, K. Zhang and Z. Yang, *ACS Appl. Bio Mater.*, 2021, **4**, 5212–5221.
16 S. Paul, S. Pan, A. Chakraborty, P. De and A. Mukherjee, *ACS Appl. Polym. Mater.*, 2021, **3**, 2310–2315.
17 H. A. J. Hibbard and M. M. Reynolds, *ACS Appl. Bio Mater.*, 2020, **3**, 5367–5374.
18 K. Zhang, H. Xu, X. Jia, Y. Chen, M. Ma, L. Sun and H. Chen, *ACS Nano*, 2016, **10**, 10816–10828.
19 A. Ratnam, S. Kumari, S. Singh, K. Mawai, R. Kumar, U. P. Singh and K. Ghosh, *J. Coord. Chem.*, 2022, **75**, 2933–2943.
20 E. T. Everett, *J. Dent. Res.*, 2010, **90**, 552–560.
21 J. Hamel, *Crit. Care Nurse*, 2011, **31**, 72–82.
22 Z.-B. Zheng, Q.-Y. Huang, Y.-F. Han, J. Zuo and Y.-N. Ma, *Sens. Actuators, B*, 2017, **253**, 203–212.
23 S. Li, C. Zhang, S. Huang, F. Hu, J. Yin and S. H. Liu, *RSC Adv.*, 2012, **2**, 4215–4219.
24 C. Sierra, B. Castro Agudelo, C. Ochoa-Puentes, W. Rodriguez-Cordoba and A. Reiber, *Rev. Colomb. Quim.*, 2018, **47**, 77–85.
25 J. Akl, I. Sasaki, P. G. Lacroix, I. Malfant, S. Mallet-Ladeira, P. Vicendo, N. Farfán and R. Santillan, *Dalton Trans.*, 2014, **43**, 12721–12733.
26 K. Karidi, A. Garoufis, A. Tsipis, N. Hadjiliadis, H. den Dulk and J. Reedijk, *Dalton Trans.*, 2005, 1176–1187, DOI: **10.1039/B418838A**.
27 T. Hirano, K. Ueda, M. Mukaida, H. Nagao and T. Oi, *J. Chem. Soc., Dalton Trans.*, 2001, 2341–2345, DOI: **10.1039/B101546J**.
28 H. Nagao, K. Enomoto, Y. Wakabayashi, G. Komiya, T. Hirano and T. Oi, *Inorg. Chem.*, 2007, **46**, 1431–1439.
29 B. Cormary, S. Ladeira, K. Jacob, P. G. Lacroix, T. Woike, D. Schaniel and I. Malfant, *Inorg. Chem.*, 2012, **51**, 7492–7501.
30 J. Akl, I. Sasaki, P. G. Lacroix, V. Hugues, P. Vicendo, M. Bocé, S. Mallet-Ladeira, M. Blanchard-Desce and I. Malfant, *Photochem. Photobiol. Sci.*, 2016, **15**, 1484–1491.
31 I. Muñoz Resta and F. Galindo, *Dyes Pigm.*, 2022, **197**, 109908.
32 R. Sakla, A. Singh, R. Kaushik, P. Kumar and D. A. Jose, *Inorg. Chem.*, 2019, **58**, 10761–10768.
33 R. E. Hintze and P. C. Ford, *J. Am. Chem. Soc.*, 1975, **97**, 2664–2671.
34 S. K. Padhan, M. B. Podh, P. K. Sahu and S. N. Sahu, *Sens. Actuators, B*, 2018, **255**, 1376–1390.
35 P. Kumar, A. Ghosh and D. A. Jose, *ChemistrySelect*, 2021, **6**, 820–842.
36 P. Kumar, R. Sakla, A. Ghosh and D. A. Jose, *ACS Appl. Mater. Interfaces*, 2017, **9**, 25600–25605.
37 M. Boiocchi, L. Del Boca, D. E. Gómez, L. Fabbrizzi, M. Licchelli and E. Monzani, *J. Am. Chem. Soc.*, 2004, **126**, 16507–16514.
38 T. P. Martyanov, A. A. Kudrevatykh, E. N. Ushakov, D. V. Korchagin, I. V. Sulimenkov, S. G. Vasil'ev, S. P. Gromov and L. S. Klimenko, *Tetrahedron*, 2021, **93**, 132312.
39 K. L. Moffa, C. N. Teahan, C. L. Montgomery, S. L. Shepherd, J. C. Dickenson, K. R. Benson, M. Olsen, W. J. Boyko, M. Bezpalko, W. S. Kassel, T. J. Dudley, D. P. Harrison and J. J. Paul, *Polyhedron*, 2023, **244**, 116582.
40 Y. Juarez-Martinez, P. Labra-Vázquez, P. G. Lacroix, M. Tassé, S. Mallet-Ladeira, V. Pimienta and I. Malfant, *Inorg. Chem.*, 2024, **63**, 7665–7677.

41 I. A. Yakovlev, J. A. Golubeva, L. S. Klyushova, V. A. Nadolinny, G. A. Kostin and A. A. Mikhailov, *ChemPhotoChem*, 2024, **8**, e202300292.
42 R. Kaushik, A. Ghosh and D. A. Jose, *J. Lumin.*, 2016, **171**, 112–117.
43 N. Sharma, D. A. Jose, N. Jain, S. Parmar, A. Srivastav, J. Chawla, A. R. Naziruddin and C. R. Mariappan, *Langmuir*, 2022, **38**, 13602–13612.
44 Y. Qu, J. Hua and H. Tian, *Org. Lett.*, 2010, **12**, 3320–3323.